Carbohydrate Polymers 87 (2012) 2538–2545

Contents lists available at SciVerse ScienceDirect

Carbohydrate Polymers

journal homepage: www.elsevier.com/locate/carbpol

Optimum conditions for lipase immobilization on chitosan-coated Fe_3O_4 nanoparticles

Chia-Hung Kuo[a], Yung-Chuan Liu[b], Chieh-Ming J. Chang[b], Jiann-Hwa Chen[c], Cheng Chang[a], Chwen-Jen Shieh[a,*]

[a] Biotechnology Center, National Chung Hsing University, 250, Kuo Kuang Road, Taichung 402, Taiwan
[b] Department of Chemical Engineering, National Chung Hsing University, Taichung 402, Taiwan
[c] Graduate Institute of Molecular Biology, National Chung Hsing University, Taichung 402, Taiwan

ARTICLE INFO

Article history:
Received 3 October 2011
Received in revised form 8 November 2011
Accepted 8 November 2011
Available online 17 November 2011

Keywords:
Lipase
Magnetic Fe_3O_4
Chitosan
Immobilization
Response surface methodology (RSM)

ABSTRACT

Magnetic Fe_3O_4–chitosan nanoparticles are prepared by the coagulation of an aqueous solution of chitosan with Fe_3O_4 nanoparticles. The characterization of Fe_3O_4–chitosan is analyzed by FTIR, FESEM, and SQUID magnetometry. The Fe_3O_4–chitosan nanoparticles are used for the covalent immobilization of lipase from *Candida rugosa* using N-(3-dimethylaminopropyl)-N′-ethylcarbodiimide (EDC) and N-hydroxysuccinimide (NHS) as coupling agents. The response surface methodology (RSM) was employed to search the optimal immobilization conditions and understand the significance of the factors affecting the immobilized lipase activity. Based on the ridge max analysis, the optimum immobilization conditions were immobilization time 2.14 h, pH 6.37, and enzyme/support ratio 0.73 (w/w); the highest activity obtained was 20 U/g Fe_3O_4–chitosan. After twenty repeated uses, the immobilized lipase retains over 83% of its original activity. The immobilized lipase shows better operational stability, including wider thermal and pH ranges, and remains stable after 13 days of storage at 25 °C.

1. Introduction

Lipase (triacylglycerol ester hydrolase, EC 3.1.1.3) has many industrial applications, because it catalyzes hydrolysis of triacylglycerol into glycerol and fatty acids (Fernandez-Lafuente, 2010). In organic systems, the enzyme catalyzes the reverse synthesis reaction to produce esters (Haas, Fox, & Foglia, 2011; Krause, Hilterhaus, Fieg, Liese, & Bornscheuer, 2009). Recently, the use of lipase as a catalyst to produce biodiesel by transforming triglycerides into fatty acid alkyl esters has been reported (Li, Fan, Hu, & Wu, 2011). However, the free lipase is not favored in industrial developments because it is difficult to recover for reuse, and it has low stability. These drawbacks can be overcome by immobilization on various supports. For instance, chitosan (2-amino-2-deoxy-(1 → 4)-β-D-glucan) is a polysaccharide carrying amino groups useful for conjugation with proteins via cross-linking agents such as N-(3-dimethylaminopropyl)-N′-ethylcarbodiimide (EDC), N-hydroxysuccinimide (NHS), or glutaldehyde. Chitosan supports have been used for lipase immobilization that permits to retain at least 80% of the initial activity after 10 hydrolytic cycles (Chiou & Wu, 2004; Romdhane, Romdhane, Gargouri, & Belghith, 2011), however it should be kept in mind that chitosan can be hydrolyzed under the unspecific action of lipases (Muzzarelli, Xia, Tomasetti, & Ilari, 1995).

Enzymes immobilized on Fe_3O_4 nanoparticles have the advantage of being easily and effectively recovered by application of a magnetic field. For the covalent immobilization of enzymes, magnetic Fe_3O_4 nanoparticles need to be modified or coated with a few atomic layers of chemically active polymer to provide functional groups for linkage. Various enzymes, such as β-D-galactosidase (Zhang, Gao, & Gao, 2010), alcohol dehydrogenase (Li, Zhou, Li, Huang, & Zhong, 2010), laccase (Bayramoglu, Yilmaz, & Arica, 2010) and α-amylase (Liu, Jia, Ran, & Wu, 2010) have been immobilized onto Fe_3O_4 nanoparticles. However, lipase immobilized onto Fe_3O_4 nanoparticles via physical adsorption showed reduced stability after repeated use (Lee et al., 2009; Yong et al., 2008).

To solve this problem, the covalent immobilization method was employed to enhance the immobilized lipase stabililty in this study. Response surface methodology (RSM) is a collection of mathematical and statistical techniques for designing experiments, building models, evaluating the relative significance of several independent variables, and determining the optimum conditions for desirable responses. It is used for evaluating the effects of various parameters and their interactions in a process through a small number of experiments. RSM has been applied successfully for the optimization of parameters of various enzyme immobilized processes (Aybastier & Demir, 2010; Mukherjee, Kumar,

* Corresponding author. Tel.: +886 4 2284 0450x5121; fax: +886 4 2286 1905.
E-mail addresses: cjshieh@dragon.nchu.edu.tw, cjshieh@nchu.edu.tw (C.-J. Shieh).

0144-8617/$ – see front matter © 2011 Elsevier Ltd. All rights reserved.
doi:10.1016/j.carbpol.2011.11.026

Rai, & Roy, 2010). Compared with a one-factor-at-a-time design, which is adopted most frequently in the literature, the experimental design and RSM were more efficient in reducing the number of experimental runs and time for investigating the optimal conditions.

2. Materials and methods

2.1. Materials

Lipase from *Candida rugosa* (Amano AY-30) was purchased from Amano International Enzyme Co. (Nagoya, Japan). Ferric chloride hexahydrate ($FeCl_3{\cdot}6H_2O$) and ferrous sulfate heptahydrate ($FeSO_4{\cdot}7H_2O$) were purchased from Acros (Pittsburgh, PA). N-hydroxysuccinimide (NHS), N-(3-dimethylaminopropyl)-N′-ethylcarbodiimide hydrochloride (EDC), sodium tripolyphosphate (TPP), and bovine serum albumin were purchased from Sigma–Aldrich (St. Louis, MO). Chitosan powder (MW 140,000 Da/mol) with 90% deacetylation that had been sieved by a 100-mesh filter was obtained from Shin ERA Tech. Co. Ltd. (Taipei, Taiwan). Ammonium hydroxide (28%) was purchased from Katayama Chemical Co. Ltd. (Osaka, Japan). p-Nitrophenyl palmitate (p-NPP) and ninhydrin were purchased from Alfa Aesar (Ward Hill, MA). Unless otherwise noted, all reagents and chemicals were analytic grade.

2.2. Preparation of Fe_3O_4 and Fe_3O_4–chitosan nanoparticles

Fe_3O_4 nanoparticles were prepared by the co-precipitating method (Pan et al., 2009). Briefly, ferric chloride hexahydrate (4.05 g) and ferrous sulfate heptahydrate (4.17 g) were dissolved in 50 ml of deionized water. NH_4OH solution (28%) was added to the solution with vigorous stirring at 25 °C, and the pH was adjusted to 10. This solution was incubated at 80 °C for 30 min and then cooled to room temperature by stirring. Fe_3O_4 nanoparticles thus formed were separated magnetically and washed several times with deionized water to remove the excess ammonia. The chitosan solution was prepared by dissolving 0.5 g of chitosan in 50 ml of 1% (v/v) acetic acid, followed by the addition of 12.5 ml of 1 mg/ml TPP solution as a crosslinker to enhance colloidal stability (Hsieh et al., 2007; Muzzarelli & Muzzarelli, 2005; Wang, Dong, Du, & Kennedy, 2007) and incubation at room temperature for 10 min. The solution was used to resuspend the magnetic Fe_3O_4 nanoparticles as described above. The suspension was vigorously stirred for 30 min to ensure the even coating of the chitosan onto the nanoparticles. Twenty-five millilitre of 1 N NaOH was added slowly to the suspension to precipitate the coated nanoparticles. The resulting Fe_3O_4–chitosan nanoparticles were recovered from the suspension by applying a magnet. They were washed with deionized water several times until the pH reached 7.0, resuspended in 50 ml of deionized water, and stored at 4 °C until use. The level of Fe_3O_4–chitosan nanoparticles in the suspension was approximately 30 mg/ml.

2.3. Characterization of magnetic Fe_3O_4 and Fe_3O_4–chitosan nanoparticles

The field-emission scanning electron microscopy (FESEM) images were recorded using a Zeiss Ultra Plus field-emission microscope. The FTIR spectra of the Fe_3O_4 and Fe_3O_4–chitosan nanoparticles were obtained using an FTIR spectrophotometer (PARAGON 500, Perkin Elmer). The magnetic properties of Fe_3O_4 and Fe_3O_4–chitosan were determined at 300 K by superconducting quantum interference devices (SQUID) (SQUID, MPMS-7 Quantum Design). The amino groups of the Fe_3O_4–chitosan nanoparticles were determined by the ninhydrin method using glycine as the standard (Kaiser, Colescott, Bossinger, & Cook, 1970). Briefly, 0.1 ml of the magnetic fluid was added to a tube containing 0.2 ml of ninhydrin reagent. The solution was heated in boiling water for 3 min and diluted with 0.8 ml of EtOH. The amine concentration was determined by readings of UV absorbance at 570 nm.

2.4. Immobilization of lipase on Fe_3O_4–chitosan nanoparticles

Two milligram of EDC (2.6 mM) was added to 4 ml of 50 mM phosphate buffer solution containing 15–35 mg of lipase, and the solution was incubated at 25 °C for 1 h with shaking (150 rpm). Then, 2.4 mg of NHS (5.2 mM) was added to the solution and the incubation continued for another 1 h. The solution was then transferred to a glass tube containing 50 mg of Fe_3O_4–chitosan. In the procedure, as depicted in Fig. 1, the carboxyl groups of lipase were activated by EDC and NHS and subsequently reacted with the amino groups of the Fe_3O_4–chitosan nanoparticles.

2.5. Experimental design and data analysis

In order to evaluate the effects of immobilization time (x_1), immobilization pH (x_2), and the enzyme/support ratio (x_3) on lipase immobilization, a 3-factor and 3-level central composite design (CCD) and RSM were applied to investigate the optimum levels of these variables and their relationships. The variables and their levels selected for the study were as follows: an immobilization time of 0.5–3.5 h; an immobilization pH of 7–9; and an enzyme/support ratio of 0.3–0.7, w/w. Table 1 shows the levels of the independent factors and experimental designs as coded (0, 1, and −1) and uncoded (actual value). A total of 16 experimental runs, including combinations of different levels of the three factors, were carried out in duplicate. The experimental data (Table 1) were analyzed by response surface regression (RSREG) to fit the following second-order polynomial equation (SAS, 1990):

$$Y = \beta_{k0} + \sum_{i=1}^{3}\beta_{ki}X_i + \sum_{i=1}^{3}\beta_{kii}X_i^2 + \sum_{i=1}^{2}\sum_{j=i+1}^{3}\beta_{kij}X_iX_j \quad (1)$$

where Y is the response (activity of lipase); β_{k0}, β_{ki}, β_{kii} and βk_{ij} are constant coefficients; and X_i and X_j are uncoded independent variables. The option of ridge max was employed to compute the estimated ridge of maximum response for increasing the radius from the centre of the original design.

2.6. Determination of lipase activity and protein content

Lipase activity was determined using p-nitrophenyl palmitate (p-NPP) as the substrate. The release of p-nitrophenol resulting from the lipase-catalyzed hydrolysis of p-NPP was measured by a reading of the absorbance at 410 nm. Fifty milligram of immobilized lipase was added to a mixture of 1 ml of 0.5% (w/v) p-nitrophenyl palmitate (p-NPP) in ethanol and 1 ml of 0.05 M phosphate buffer solution (pH 7.0). The solution was incubated at 30 °C for 5 min, and 2 ml of 0.5 N Na_2CO_3 was added to terminate the reaction. After centrifuging at 10,000 rpm for 10 min, 0.5 ml of the supernatant was diluted 10-fold with distilled water and the absorbance at 410 nm was measured with a UV/VIS spectrophotometer (Metertek SP-830, Metertech Inc., Taiwan). The molar extinction coefficient (ε410) for p-nitrophenol is 15,000 $M^{-1}\,cm^{-1}$. One unit (U) of enzyme activity is defined as the amount of enzyme which liberates 1 mmol p-nitrophenol per minute under assay conditions. The protein content of the immobilized lipase was determined by the Bradford method using protein dye reagent concentrate (Bio-Rad, Hercules, California). Bovine serum albumin was used as the standard.

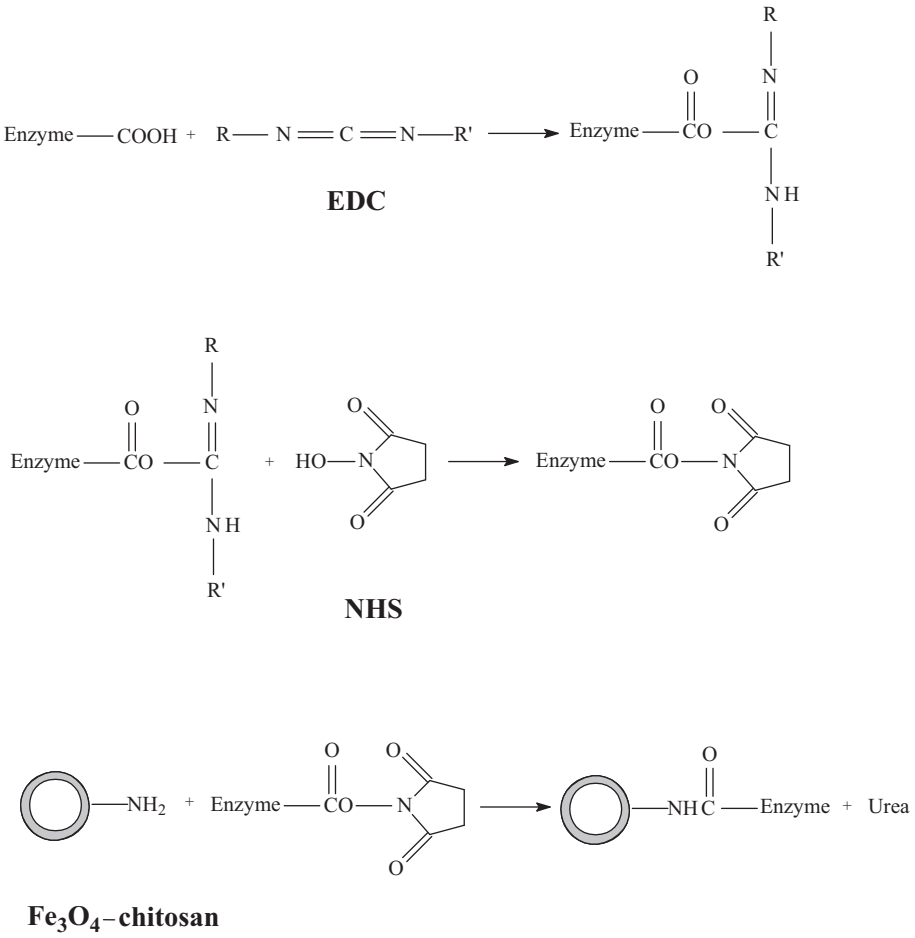

Fig. 1. Schematic presentation of lipase immobilization on Fe_3O_4–chitosan nanoparticles.

2.7. Determination of the immobilized lipase stability

The stability of the lipase (free and immobilized) was evaluated by measuring the enzyme activity before and after treatment. The activity before the treatment was assigned as 100% and the activity after the treatment was expressed as relative activity. Thermal stability was evaluated by incubating the enzyme in a water bath for 1 h at temperatures ranging from 30 to 70 °C. The pH stability of the lipase was investigated by incubating the enzyme in the phosphate buffer at pHs ranging from 3 to 11 for 1 h. Storage stability was investigated by storing the enzyme at 25 °C for a fixed period of time. The reusability of the immobilized lipase was evaluated by collecting the immobilized lipase by magnetization after one determination of the activity, washing the enzyme three times with

Table 1
Central composite design and observed experimental data for 3-level–3-factor response surface analysis.

Treatment no.	Factor			Experimental values activity (U/g)	Protein loading yield (%)
	Time (h), x_1	pH, x_2	Enzyme/support ratio (w/w), x_3		
1	−1[a](0.5)	−1 (7)	−1 (0.3)	7.95 ± 0.09	76 ± 1
2	1 (3.5)	−1 (7)	−1 (0.3)	8.84 ± 0.51	78 ± 9
3	0 (2.0)	−1 (7)	0 (0.5)	8.27 ± 0.22	72 ± 5
4	−1 (0.5)	−1 (7)	1 (0.7)	12.64 ± 0.39	51 ± 1
5	1 (3.5)	−1 (7)	1 (0.7)	13.15 ± 0.47	63 ± 6
6	0 (2.0)	0 (8)	−1 (0.3)	3.63 ± 0.70	49 ± 10
7	−1 (0.5)	0 (8)	0 (0.5)	3.26 ± 0.16	30 ± 11
8	0 (2.0)	0 (8)	0 (0.5)	5.44 ± 0.05	37 ± 4
9	0 (2.0)	0 (8)	0 (0.5)	6.02 ± 0.42	40 ± 1
10	1 (3.5)	0 (8)	0 (0.5)	4.60 ± 0.47	33 ± 0
11	0 (2.0)	0 (8)	1 (0.7)	7.93 ± 0.22	43 ± 3
12	1 (3.5)	1 (9)	−1 (0.3)	2.53 ± 0.06	29 ± 1
13	−1 (0.5)	1 (9)	−1 (0.3)	3.15 ± 0.19	31 ± 2
14	0 (2.0)	1 (9)	0 (0.5)	3.01 ± 0.74	24 ± 0
15	−1 (0.5)	1 (9)	1 (0.7)	4.04 ± 0.12	40 ± 7
16	1 (3.5)	1 (9)	1 (0.7)	2.62 ± 0.00	36 ± 0

[a] The values −1, 0, and 1 are coded levels.

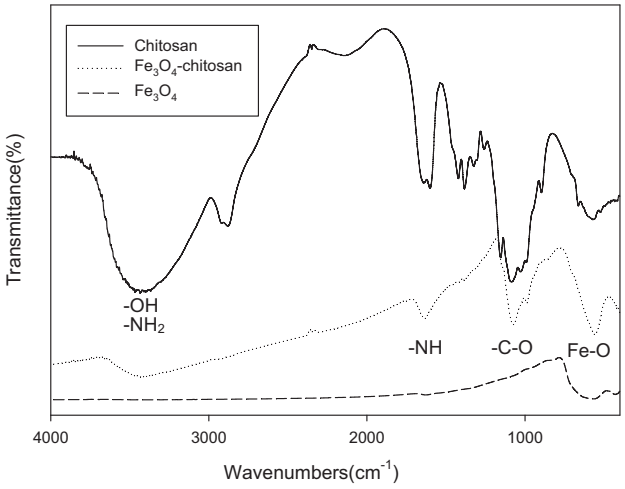

Fig. 2. FTIR spectra of chitosan, Fe_3O_4 and Fe_3O_4–chitosan nanoparticles.

a phosphate buffer (0.02 M, pH 7.0), and determining the enzyme activity again. The activity of the first run was defined as 100%, and the activity of subsequent runs expressed as relative activity.

3. Results and discussion

3.1. Characterization of Fe_3O_4–chitosan nanoparticles

The Fe_3O_4–chitosan nanoparticles were generated by adjusting the pH of the mixture containing the Fe_3O_4 particles and chitosan to precipitate chitosan onto the surface of the particles. Because the surface of iron oxide with a negative charge has an affinity toward chitosan, protonated chitosan can coat the magnetic nanoparticles via an electrostatic interaction (Zhao, Wang, Zeng, Xia, & Tang, 2009). After washing the Fe_3O_4–chitosan nanoparticles with water several times, the amino content of the Fe_3O_4–chitosan nanoparticles remained stable. This was demonstrated by the FTIR analysis of the chitosan and the Fe_3O_4 nanoparticles before and after chitosan coating. As shown in Fig. 2, the characteristic bands of pure chitosan were at 3420 (O–H stretching and N–H stretching vibrations), 1645 (amide), and 1076 cm^{-1} (C–O–C stretching vibration), consistent with a previous report (Gao et al., 2008). After chitosan coating, a band at 580 cm^{-1} relevant to the Fe–O vibration appeared in addition to all of the characteristic bands for the chitosan and Fe_3O_4 particles. This indicated a successful generation of Fe_3O_4–chitosan particles. The amino content of the Fe_3O_4–chitosan particles was determined by ninhydrin reagent to be 0.116 mmol NH_2/g Fe_3O_4–chitosan. The surface morphology of Fe_3O_4 is shown in Fig. 3A; the average size is 30 nm, and the magnetic Fe_3O_4 nanoparticles were physically aggregated. This could have been caused by the coercive force of the magnetic particles. After the coating with chitosan (Fig. 3B), the surface morphology of Fe_3O_4–chitosan showed little change, but the size of the particles became smaller since the electrostatic interaction between the Fe_3O_4 nanoparticles and chitosan in the coating process increased the repulsive force of the magnetic particles. The elemental compositions are calculated from the energy dispersive X-ray (EDX). The elemental compositions of Fe_3O_4 nanoparticles are 70.9, 26.2, and 2.8% for Fe, O, and C, respectively. However, after the coating with chitosan, the elemental compositions change to 60.1, 27.3, and 12.6%; the weight of the carbon and oxygen increased 9.8% and 0.9%, respectively. This meant at least 11% of the chitosan was coated onto the surface of the Fe_3O_4 nanoparticles.

The magnetic properties of the Fe_3O_4 and Fe_3O_4–chitosan nanoparticles were studied by SQUID analysis. Fig. 4 shows their

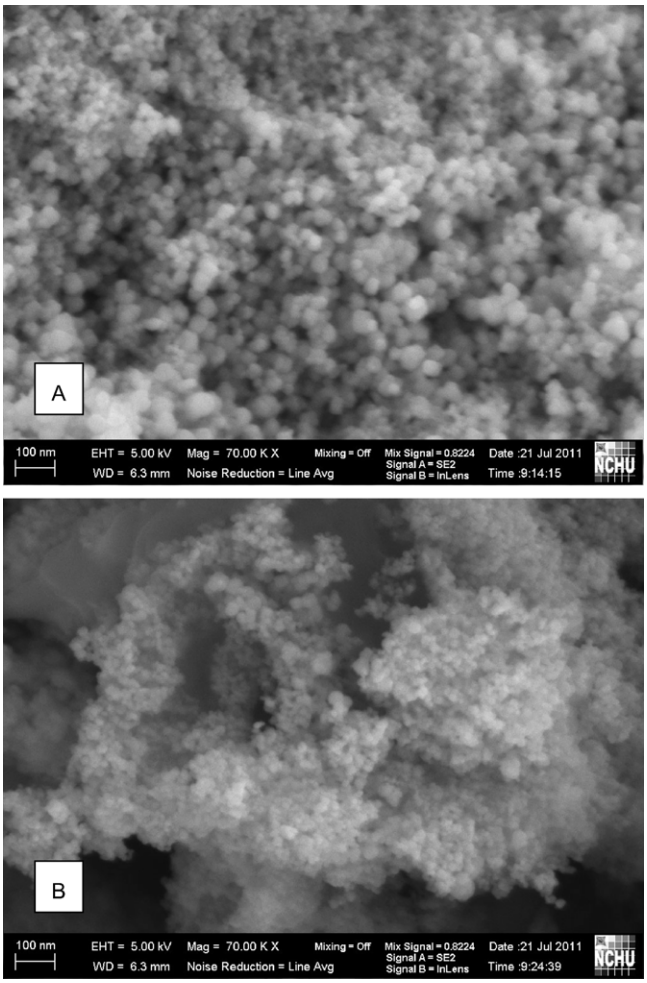

Fig. 3. Field emission scanning electron microscopy (FESEM) images of magnetic nanoparticles (A) Fe_3O_4; (B) Fe_3O_4–chitosan.

magnetization hysteresis loops. The saturation magnetization was 60.00 emu/g for Fe_3O_4–chitosan, which was 25% lower than that for Fe_3O_4 (80.89 emu/g). This decrease in the saturation magnetization of the Fe_3O_4–chitosan nanoparticles was likely due to the increase in the mass of the Fe_3O_4–chitosan nanoparticles from the chitosan coating. The magnetization curves for both Fe_3O_4 and

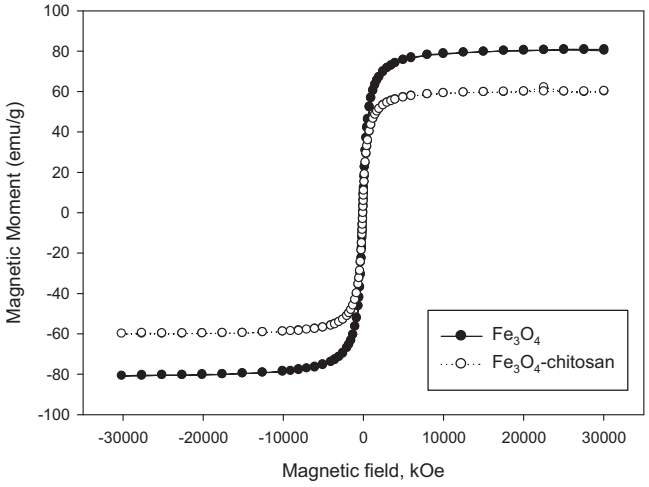

Fig. 4. Hysteresis loops of Fe_3O_4 and Fe_3O_4–chitosan measured at 300 K.

Fe_3O_4–chitosan crossed the zero point in the SQUID plot (Fig. 4), indicating that the nanoparticles of both were super-paramagnetic.

3.2. Immobilization of lipase and the immobilization variables

NHS and EDC were used for the immobilization of lipase onto the Fe_3O_4–chitosan nanoparticles. EDC can activate carboxyl groups and is used frequently in peptide synthesis, enzyme immobilization, and the cross-linking of proteins to nucleic acids (Hong et al., 2007; Thomson et al., 1995). It was hypothesized that the carboxyl groups of lipase could be activated by EDC to form an unstable enzyme–EDC complex. In the presence of NHS, an ester between lipase and NHS would form and react with the amino groups on the Fe_3O_4–chitosan nanoparticles. Fig. 1 depicts this hypothesis. Three parameters, i.e., immobilization time, immobilization pH and enzyme/support ratio, were chosen and their respective influence was investigated by analyzing the immobilized lipase activity in each of the 16 immobilization experiments, designed by a 3-level-3-factor CCD and RSM. The results are shown in Table 1. Of the 16 experiments, the experiment of treatment #5 (3.5 h, pH 7 and enzyme/support ratio 0.7) had the greatest immobilized lipase activity (13.15 U/g Fe_3O_4–chitosan), whereas the experiment of treatment #12 (3.5 h, pH 9 and enzyme/support ratio 0.3) had the least activity (2.53 U/g Fe_3O_4–chitosan). From the SAS output of the RSREG procedure, the second-order polynomial Eq. (2) is given below:

$$Y = 84.511516 + 3.588175x_1 - 18.717729x_2 + 16.170518x_3 - 0.253342x_1x_1 - 0.285209x_2x_1 + 1.140381x_2x_2 - 0.492178x_3x_1 - 5.012933x_3x_2 + 32.056184x_3x_3 \quad (2)$$

where Y is the immobilized lipase activity (U/g Fe_3O_4–chitosan), x_1 is the immobilization time, x_2 is the immobilization pH, and x_3 is the enzyme/support ratio.

By ANOVA analysis, this quadratic polynomial model was highly significant and sufficient to represent the actual relationship between the response and the three parameters with a very low p-value (0.0015) and a satisfactory coefficient of determination ($R^2 = 0.96$). Therefore, this model was adequate to predict the immobilization results within the range of the variables employed.

3.3. Relationships between immobilization factors and response

Using surface response plots of the quadric polynomial model, the relationships between the immobilization factors and the response (immobilized lipase activity) could be better understood by holding one variable constant and studying the function between the other two variables. Fig. 5A shows the effects of pH, immobilization time, and their mutual interaction on the immobilization at an enzyme/support ratio of 0.7; whereas Fig. 5B shows the effects of the enzyme/support ratio, immobilization time, and their mutual interaction on the immobilization at pH 7. With a fixed immobilization time anywhere between 0.5 and 3.5 h, a decrease in pH (from 9 to 7) and an increase in the enzyme/support ratio (from 0.3 to 0.7) led to an increase in lipase activity (from 3.0 to 13.0 U/g Fe_3O_4–chitosan and from 7.2 to 12.8 U/g Fe_3O_4–chitosan, respectively). The immobilization pH and enzyme/support ratio appeared to be important in the immobilization. However, immobilization time had little effect on the immobilization. Fig. 5C shows the combination effects of pH and the enzyme/support ratio on the immobilized lipase activity under a fixed immobilization time of 2 h. Decreasing the immobilization pH to 7 and increasing the enzyme/support ratio to 0.7 resulted in maximal immobilized lipase activity (over 13 U/g Fe_3O_4–chitosan). On the other hand, increasing the immobilization pH to 9 and decreasing the enzyme/support ratio to 0.3 resulted in minimal immobilized lipase activity (2.5–4 U/g Fe_3O_4–chitosan). It was concluded that the immobilization pH and enzyme/support ratio were the most important parameters in this immobilization process and could be considered as indicators of effectiveness.

The protein loading was calculated from the protein concentration change in the enzyme solution before and after immobilization. Table 1 shows the yields of the protein loading on the Fe_3O_4–chitosan nanoparticles in the 16 immobilization experiments. The increase in the immobilization pH correlated well to a decrease in the protein loading yield, because the EDC and NHS were less active in an alkaline solution. Thus, lower protein loading led to the lower immobilized lipase activity obtained at pH 9.

3.4. Attaining optimum immobilization condition

The optimum immobilization conditions were determined by ridge max analysis, which computed the estimated ridge of maximum response for an increasing radius from the centre of the original design (SAS, 1990). The immobilized lipase activity (response; Y) at distances of 0, 1.4, 2.0, 2.5 and 3.0 was calculated according to the immobilization model [Eq. (2)] shown in Table 2. The actual experimental value of the lipase activity increasing as the radius distance increased and reached the maximum at a radius distance of 2.0. With a radius distance greater than 2.0, lipase activity gradually decreased as the radius distance increased. When the radius distance was over 2.0, the experimental pH was 6.0 and 5.64, E/S ratio was 0.8 and 0.87 (corresponding to radius distances of 2.5 and 3.0). However, decreasing the pH and increasing the E/S ratio led to the protein over loading on the surface of the Fe_3O_4–chitosan nanoparticles. The over loading of protein might cause enzyme aggregation, decreasing the lipase activity. Based on the ridge max analysis, the maximum immobilization conditions could be obtained at an immobilization time of 2.14 h, an immobilization pH of 6.37, and an enzyme/support ratio of 0.73, with maximal lipase activity of 19.96 ± 0.60 U/g Fe_3O_4–chitosan. In other words, the ridge max analysis showed an increase of at least 50% in lipase activity, as compared with the maximum lipase activity in Table 1 experiment.

3.5. Hydrolytic stability of immobilized lipase

To understand the reusability of the immobilized Fe_3O_4–chitosan particles, the lipase activity of the particles was determined after repeated use. Lipase was immobilized onto Fe_3O_4–chitosan nanoparticles under the optimum conditions. The activity of the immobilized lipase was determined after each of

Table 2
Estimated ridge of maximum response Y (lipase activity; U/g Fe_3O_4–chitosan).

Coded radius	Time, x_1	pH, x_2	E/S ratio, x_3	Estimated activity	Experimental activity
0.0	2.00	8.00	0.50	4.90 ± 0.51	5.73 ± 0.29
1.4	2.10	6.83	0.65	13.39 ± 0.98	15.20 ± 0.83
2.0	2.14	6.37	0.73	19.02 ± 1.82	19.96 ± 0.60
2.5	2.18	6.00	0.80	24.64 ± 2.78	18.89 ± 0.09
3.0	2.21	5.64	0.87	31.11 ± 3.95	13.47 ± 1.90

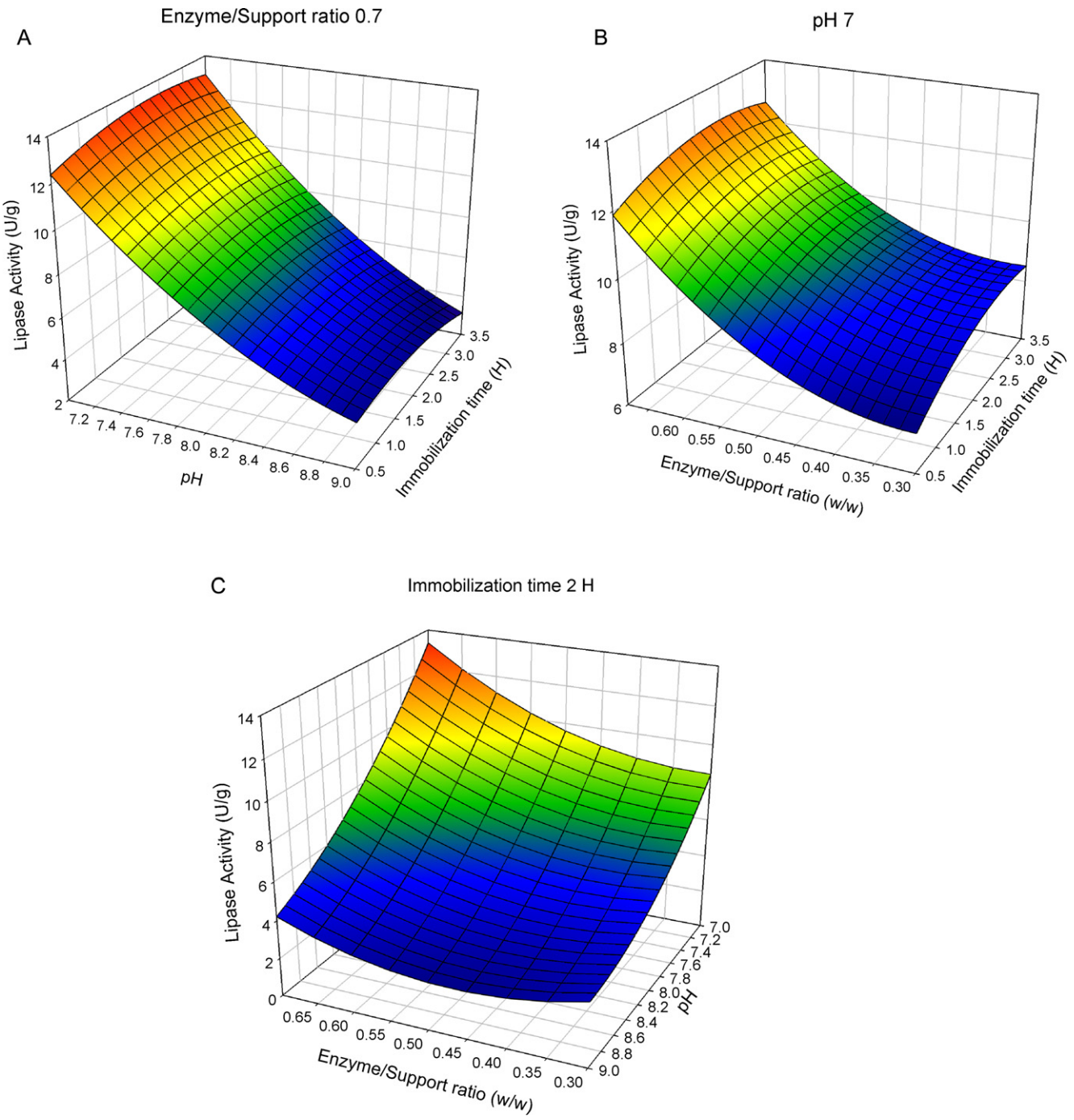

Fig. 5. Response surface plots show (A) the effect of pH, immobilization time, and their mutual interaction on immobilized lipase; (B) the effect of E/S ratio and immobilization time; and (C) the effect of E/S ratio, pH, and their mutual interaction on the immobilized lipase.

the 20 repeated recoveries and uses. As shown in Fig. 6A, after 5, 10 and 20 repeated recovery and uses, the immobilized lipase retained about 98%, 88% and 83% of the original activity, respectively. The gradual yet slight decrease in enzyme activity could be attributed to the denaturation and/or leakage of lipase from the supports. With this excellent reusability and ease of recovery (by simple magnetic separation), the immobilized lipase prepared under the optimum conditions would be of great use in industrial applications.

The thermal stability of both the immobilized and free lipase was studied by incubating the immobilized lipase, prepared under the optimum conditions, at 30, 40, 50, and 60 °C for 1 h and then measuring the lipase activity. As shown in Fig. 6B, the immobilized lipase retained its full activity after incubation at 30 °C, 40 °C and 50 °C for 1 h. Under the same incubation conditions, the activity of the free enzyme, however, decreased linearly as the incubation temperature increased. After incubation at 60 °C for 1 h, the free and immobilized lipase retained 21% and 76%, respectively, of the original activity. The immobilized lipase was much more heat-stable than the free lipase.

The pH stability of the free and immobilized lipases was determined by dissolving each of the two lipases in 50 mM of phosphate buffer with a pH of 3–11 for 1 h at 25 °C and then measuring the lipase activity in the pH 7 buffer. The results are shown in Fig. 6C.

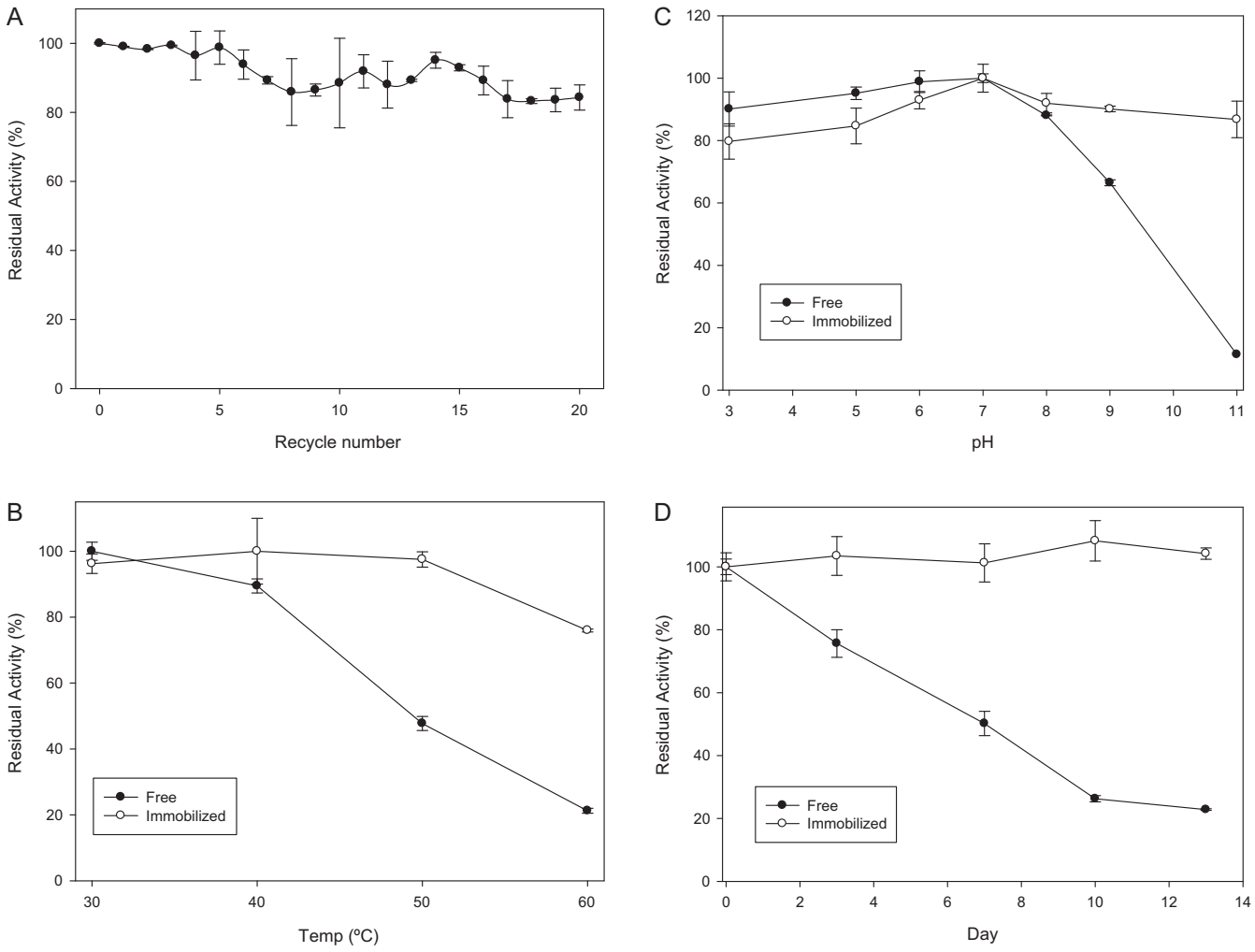

Fig. 6. (A) Reuse, (B) thermal, (C) pH, and (D) storage stability of lipase immobilized on magnetic Fe_3O_4–chitosan nanoparticles.

The free lipase was stable in buffers of pH 3, 4, 5, 6, 7, and 8. In buffers of pH 9 and 11, the free lipase retained only about 70% and 10%, respectively, of the original activity. On the other hand, the immobilized lipase retained its full activity in buffers of all pHs. The immobilization clearly improved the thermal and pH stabilities of the lipase.

The storage stability of the immobilized lipase prepared under the optimum conditions was also investigated. The free and immobilized lipases in phosphate buffers of pH 7 were stored at 25 °C for 3, 7, 10 and 13 days, and the activities were determined. As shown in Fig. 6D, the immobilized lipase retained its full activity under all storage conditions, whereas the free lipase gradually lost its activity as the storage time increased. It has been reported that immobilized enzymes, particularly covalently immobilized enzymes, are more resistant to high temperatures or extreme pHs than soluble enzymes (Chiou & Wu, 2004; Hong et al., 2007; Yiitolu & Temoçin, 2010). It was concluded that the immobilized lipase exhibited a better operational stability, as compared to the free lipase.

4. Conclusions

Magnetic Fe_3O_4 nanoparticles coated with chitosan were prepared successfully and used for the covalent immobilization of lipase on the surface. Lipase was covalently bound to the magnetic Fe_3O_4–chitosan nanoparticles via EDC and NHS activation at room temperature. A second-order model depicting the relationship between the response (immobilized lipase activity) and the three immobilization parameters was established. The immobilized pH and enzyme/support ratio are the most significant process variables that affected the immobilized lipase activity. Based on the model, the optimum conditions for immobilization were predicted to be an immobilization time of 2.14 h, an immobilization pH of 6.37, and an enzyme/support ratio of 0.73 (w/w), and the actual immobilized lipase activity to be 19.96 ± 0.60 U/g Fe_3O_4–chitosan. Operational stability test demonstrated the immobilized lipase increased its reuse, thermal, pH, and storage stability than that of the native enzyme. It was also noticed that the immobilized lipase based on Fe_3O_4–chitosan nanoparticles was easily prepared. Taking the above results into consideration, Fe_3O_4–chitosan nanoparticles have been proving to be an efficient support for lipase immobilization.

Acknowledgment

This research was supported by the National Science Council, Taiwan, ROC (NSC-98-2313-B-005-027-MY3).

References

Aybastier, T., & Demir, C. (2010). Optimization of immobilization conditions of *Thermomyces lanuginosus* lipase on styrene-divinylbenzene copolymer using response surface methodology. *Journal of Molecular Catalysis B: Enzymatic*, *63*(3–4), 170–178.

Bayramoglu, G., Yilmaz, M., & Arica, M. Y. (2010). Preparation and characterization of epoxy-functionalized magnetic chitosan beads: Laccase immobilized for degradation of reactive dyes. *Bioprocess and Biosystems Engineering*, *33*(4), 439–448.

Chiou, S. H., & Wu, W. T. (2004). Immobilization of *Candida rugosa* lipase on chitosan with activation of the hydroxyl groups. *Biomaterials*, *25*(2), 197–204.

Fernandez-Lafuente, R. (2010). Lipase from *Thermomyces lanuginosus*: Uses and prospects as an industrial biocatalyst. *Journal of Molecular Catalysis B: Enzymatic*, *62*(3–4), 197–212.

Gao, L., Wu, J., Lyle, S., Zehr, K., Cao, L., & Gao, D. (2008). Magnetite nanoparticle-linked immunosorbent assay. *Journal of Physical Chemistry C*, *112*(44), 17357–17361.

Haas, M. J., Fox, P. S., & Foglia, T. A. (2011). Lipase-catalyzed synthesis of partial acylglycerols of acetoacetate. *European Journal of Lipid Science and Technology*, *113*(2), 168–179.

Hong, J., Xu, D., Gong, P., Sun, H., Dong, L., & Yao, S. (2007). Covalent binding of α-chymotrypsin on the magnetic nanogels covered by amino groups. *Journal of Molecular Catalysis B: Enzymatic*, *45*(3–4), 84–90.

Hsieh, C. Y., Tsai, S. P., Ho, M. H., Wang, D. M., Liu, C. E., Hsieh, C. H., et al. (2007). Analysis of freeze-gelation and cross-linking processes for preparing porous chitosan scaffolds. *Carbohydrate Polymers*, *67*(1), 124–132.

Kaiser, E., Colescott, R. L., Bossinger, C. D., & Cook, P. I. (1970). Color test for detection of free terminal amino groups in the solid-phase synthesis of peptides. *Analytical Biochemistry*, *34*(2), 595–598.

Krause, P., Hilterhaus, L., Fieg, G., Liese, A., & Bornscheuer, U. (2009). Chemically and enzymatically catalyzed synthesis of C6–C10 alkyl benzoates. *European Journal of Lipid Science and Technology*, *111*(2), 194–201.

Lee, D. G., Ponvel, K. M., Kim, M., Hwang, S., Ahn, I. S., & Lee, C. H. (2009). Immobilization of lipase on hydrophobic nano-sized magnetite particles. *Journal of Molecular Catalysis B: Enzymatic*, *57*(1–4), 62–66.

Li, S. F., Fan, Y. H., Hu, R. F., & Wu, W. T. (2011). Pseudomonas cepacia lipase immobilized onto the electrospun PAN nanofibrous membranes for biodiesel production from soybean oil. *Journal of Molecular Catalysis B: Enzymatic*, *72*(1–2), 40–45.

Li, G. Y., Zhou, Z. D., Li, Y. J., Huang, K. L., & Zhong, M. (2010). Surface functionalization of chitosan-coated magnetic nanoparticles for covalent immobilization of yeast alcohol dehydrogenase from *Saccharomyces cerevisiae*. *Journal of Magnetism and Magnetic Materials*, *322*(24), 3862–3868.

Liu, Y., Jia, S., Ran, J., & Wu, S. (2010). Effects of static magnetic field on activity and stability of immobilized α-amylase in chitosan bead. *Catalysis Communications*, *11*(5), 364–367.

Mukherjee, A. K., Kumar, T. S., Rai, S. K., & Roy, J. K. (2010). Statistical optimization of Bacillus alcalophilus α-amylase immobilization on iron-oxide magnetic nanoparticles. *Biotechnology and Bioprocess Engineering*, *15*(6), 984–992.

Muzzarelli, R. A. A., & Muzzarelli, C. (2005). Chitosan chemistry: Relevance to the biomedical sciences. *Advances in Polymer Science*, *186*, 151–209.

Muzzarelli, R. A. A., Xia, W., Tomasetti, M., & Ilari, P. (1995). Depolymerization of chitosan and substituted chitosans with the aid of a wheat germ lipase preparation. *Enzyme and Microbial Technology*, *17*(6), 541–545.

Pan, C., Hu, B., Li, W., Sun, Y., Ye, H., & Zeng, X. (2009). Novel and efficient method for immobilization and stabilization of β-D-galactosidase by covalent attachment onto magnetic Fe_3O_4–chitosan nanoparticles. *Journal of Molecular Catalysis B: Enzymatic*, *61*(3–4), 208–215.

Romdhane, I. B. B., Romdhane, Z. B., Gargouri, A., & Belghith, H. (2011). Esterification activity and stability of *Talaromyces thermophilus* lipase immobilized onto chitosan. *Journal of Molecular Catalysis B: Enzymatic*, *68*(3–4), 230–239.

SAS. (1990). *SAS user guide*. Cary, NC: SAS Institute.

Thomson, S. A., Josey, J. A., Cadilla, R., Gaul, M. D., Fred Hassman, C., Luzzio, M. J., et al. (1995). Fmoc mediated synthesis of peptide nucleic acids. *Tetrahedron*, *51*(22), 6179–6194.

Wang, Q., Dong, Z., Du, Y., & Kennedy, J. F. (2007). Controlled release of ciprofloxacin hydrochloride from chitosan/polyethylene glycol blend films. *Carbohydrate Polymers*, *69*(2), 336–343.

Yiitolu, M., & Temoçin, Z. (2010). Immobilization of *Candida rugosa* lipase on glutaraldehyde-activated polyester fiber and its application for hydrolysis of some vegetable oils. *Journal of Molecular Catalysis B: Enzymatic*, *66*(1–2), 130–135.

Yong, Y., Bai, Y., Li, Y. F., Lin, L., Cui, Y., & Xia, C. (2008). Preparation and application of polymer-grafted magnetic nanoparticles for lipase immobilization. *Journal of Magnetism and Magnetic Materials*, *320*(19), 2350–2355.

Zhang, S., Gao, S., & Gao, G. (2010). Immobilization of β-galactosidase onto magnetic beads. *Applied Biochemistry and Biotechnology*, *160*(5), 1386–1393.

Zhao, D. L., Wang, X. X., Zeng, X. W., Xia, Q. S., & Tang, J. T. (2009). Preparation and inductive heating property of Fe_3O_4–chitosan composite nanoparticles in an AC magnetic field for localized hyperthermia. *Journal of Alloys and Compounds*, *477*(1–2), 739–743.